CONSTITUTIVE BEHAVIOUR OF HYBRID FERRO FIBER CONCRETE (HFFC) UNDER AXIAL COMPRESSION

K.Ramesh* D.R.Seshu and M.Prabhakar*****

The combination of fiber reinforced concrete and ferrocement can be made use in developing a concrete composite with adequate ductility, which is required in structures subjected to seismic forces. Such concrete composite can be termed as HYBRID FERRO FIBER CONCRETE (HFFC). This paper presents an analytical model for predicting the stress-strain behavior of hybrid ferro fiber concrete (HFFC), based on the experimental results. A total of 168 prism specimens of size 150X150X300mm were tested under strain control rate of loading. The increases in strength and strain of HFFC were used in formulating the constitutive relation.

LIST OF SYMBOLS

b, d	=	Lateral dimensions of prism
f_y	=	Yield strength of longitudinal / tie / fiber / mesh wire (Table 1)
A_s	=	Area of longitudinal steel
f_c'	=	Strength of unconfined concrete
ε_c	=	Strain at peak of unconfined concrete
f_u	=	Strength of tie confined fiber reinforced concrete (CFRC)
	=	$f_c'(1 + 0.55C_i)(1.0228 + 0.1024(RI))$
ε_u	=	Strain at ultimate of tie confined fiber reinforced concrete [13,14]
A_g	=	Gross cross-sectional area
C_i	=	Confinement index [10] $= (P_b - P_{bb})(f_v / f_c')\sqrt{(b/s)}$
P_b	=	Ratio of volume of transverse steel to the volume of concrete
P_{bb}	=	Ratio of volume of transverse steel to the volume of concrete Corresponding to a limiting pitch equal to 1.5 b
f_v	=	Stress in lateral ties
s	=	Spacing of lateral ties
ε_{fu}	=	Strain at peak of HFFC
$\varepsilon_{0.85fu}$	=	Strain at 85% of peak of HFFC in the descending portion of stress-strain curve
K_f	=	Load ratio explained in the paper
f_u'	=	Peak strength of HFFC
RI	=	Product of mass fraction of fiber (W_f) and aspect ratio of fibers
W_f	=	Ratio of mass of steel fiber and mass of concrete
S_f	=	Specific surface factor

* Research scholar, Dept. Civil Engineering, Regional Engineering College, Warangal – 506 004, India.
** Assistant Professor, Department of Civil Engineering. National Institute of Technology, Warangal – 506 004, India. E-mail:<drseshu@recw.ernet.in>
*** Professor of civil Engineering and Principal at KITS, Warangal – 506 015, India.

f = Compressive stress in HFFC
ε = Compressive strain in HFFC

INTRODUCTION

Seismic design of structures demands high ductility. The ductility of concrete may be improved by confining it in steel binders, as ties in compression members and as stirrups in beams. It has been reported [3] that a concrete strain of 0.01 is sufficient to give full redistribution of moments, thus allowing the use of plastic analysis for of concrete structures. However, the higher the degree of indeterminacy of a structure is more will be the concrete strain at failure and, hence the ductility demands at the first plastic hinge which will form in the structure. The critical section in statically indeterminate structures at which first hinge forms are usually the sections having maximum shear force. The stirrup reinforcement provided has to take care of the shear at that section and simultaneously provide confinement. It has been established [12] that only the stirrup reinforcement provided beyond what is required for resisting shear failure will only provide confinement. With practical minimum spacing that can be provided at the critical sections, there is a limit to the extent of confinement. In columns, confinement using closely spaced ties not only interrupts the continuity and creates plane of weakness between the core and the concrete cover, it also adds to the problem of reinforcement congestion. In view of the above, it may not be possible to sufficiently confine the structure by providing the laterals alone. It would be useful if a supplementary confinement in addition to the laterals, can be provided at the critical sections or a better alternative to the existing methods of confinement can be devised. Recent studies [5,13,14] conducted on confined fiber-reinforced concrete, indicated improvement in ductility. However, the investigations on FRC highlighted the limitation to the quantity of passive confinement offered by steel fibers due to balling of fibers at higher dosages. Alternatively, ferrocement shell (casing) can be used to further improve the confinement of FRC. The concrete in which the engineered use of Ferrocement and FRC is made, can be termed as Hybrid Ferro Fiber Concrete (HFFC). Author's study on the behavior of HFFC under axial compression demonstrated large improvement in ductility and at the same time dimensional stability was preserved in the post-ultimate region. This paper presents the development of characteristic stress-strain curve based on the observed behavior of HFFC under axial compression.

EXPERIMENTAL STUDY

Scheme of experimental work

The experimental program was designed to study the behavior of HFFC under axial compression by testing prisms of size 150 X 150 X 300mm. The variables in the study are specific surface factor (S_f), which controls the behavior of ferrocement, reinforcing index (RI) of steel fibers, which controls the behavior of core fiber reinforced concrete and the amount of lateral tie confinement (C_i)[10]. Specific surface factor is the product of specific surface ratio and yield stress of mesh wires in the direction of force divided by the strength of plain mortar [11]. Specific surface ratio is the ratio of the total surface area of contact of reinforcement wires present per unit length of the specimen in the direction of the application of the load in a given width and thickness of ferrocement shell to the volume of mortar. The reinforcing index (RI) of the steel fibers is the product of mass fraction (W_f) of steel fibers and the aspect ratio of the fibers. The mass fraction (W_f) is the ratio of mass of steel fibers and mass of concrete.

The program consisted of testing of 168 prisms, which were cast in 10 batches (viz., A, B, C, D, E, F, G, H and I - series). The prisms in each batch (i.e., A0 - A4 to F0 - F4) are divided into six sets. The prisms in each batch (i.e., G0 - G4 to I0 - I4) are divided into five sets. In both the cases, first set consist of plain concrete prisms and in the second set, fiber reinforced concrete prisms without any ferrocement shell as additional confinement were cast. In the remaining sets, fiber reinforced concrete prisms with ferrocement shell as additional confinement (HFFC prisms) were cast. Except in first set, the amount of reinforcement (longitudinal and lateral steel) was maintained constant and equal to that provided in the prisms of second set. However, the amount of ferrocement shell confinement varied by varying the specific surface factor (S_f). Since the effect of confinement on fiber reinforced concrete due to lateral reinforcement [13,14] was already known, the effect of confinement due to ferrocement shell can be separated. The details of prisms tested are given in Table. 1.

Materials

The galvanized woven wire mesh of square grid fabric was used in ferrocement. The ties and longitudinal steel used in the prisms were made of mild steel and galvanized iron steel, respectively. The cement used was ordinary Portland cement of 43 [7] grade conforming to IS 8112 - 1981. Machine-crushed hard granite chips passing through 12.5 mm IS sieve and retained on 4.75 mm IS sieve was used as coarse aggregate throughout the work. River sand procured locally was used for fine aggregate. Fine aggregate passing through 2.36 mm IS sieve was used in core fiber reinforced concrete and fine aggregate passing through 1.18 mm IS Sieve was used in ferrocement shell. The concrete used in the study has the mix proportion of (1:1.8:2.5 by mass and water-cement ratio = 0.5). The mortar used for the ferrocement shell has the mix proportion of one part cement and two parts sand (i.e., 1:2) with a water-cement ratio of 0.6. The water-cement ratio of 0.6 for the mortar has been adopted to enable the easy penetration of the mortar in to the mesh layers.

Preparation of specimen

After the fabrication of ferrocement cages using ties and longitudinal steel, a sufficient number of wire mesh layers to provide the required S_f were wrapped over the ties tightly. The mesh was stitched thrice so as not to fail by splitting of the mesh. Fig. 1(a) shows the reinforcement details of specimen. Fig. 1(b) shows the mold used for casting the prisms.

Table 1 Detail of Prisms Tested

S.No	Specimen Designation	Lateral Reinforcement			Longitudinal reinforcement		Mesh Reinforcement					Steel Fiber		f_c' (Mpa)	ε_c' 10^{-5}
		Dia. (mm)	f_y (Mpa)	C_i	Dia. (mm)	f_y (Mpa)	Dia. (mm)	f_y (Mpa)	Spacing (mm)	No.of Layers	S_f	V_f %	RI		
1	A0	6.42	300	0.35	4.00	390	0.33	370	1.78	0	0	0	0	23.06	160
2	A1	6.42	300	0.35	4.00	390	0.33	370	1.78	1	4.5	0	0	23.06	160
3	A2	6.42	300	0.35	4.00	390	0.33	370	1.78	2	9.0	0	0	23.06	160
4	A3	6.42	300	0.35	4.00	390	0.33	370	1.78	3	13.5	0	0	23.06	160
5	A4	6.42	300	0.35	4.00	390	0.33	370	1.78	4	18.0	0	0	23.06	160
6	B0	6.42	300	0.39	4.00	390	0.33	370	1.78	0	0	0.6	1.48	20.1	165
7	B1	6.42	300	0.39	4.00	390	0.33	370	1.78	1	4.5	0.6	1.48	20.1	165
8	B2	6.42	300	0.39	4.00	390	0.33	370	1.78	2	9.0	0.6	1.48	20.1	165
9	B3	6.42	300	0.39	4.00	390	0.33	370	1.78	3	13.5	0.6	1.48	20.1	165
10	B4	6.42	300	0.39	4.00	390	0.33	370	1.78	4	18.0	0.6	1.48	20.1	165
11	C0	6.42	300	0.37	4.00	390	0.33	370	1.78	0	0	1.2	2.96	21.74	162
12	C1	6.42	300	0.37	4.00	390	0.33	370	1.78	1	4.5	1.2	2.96	21.74	162
13	C2	6.42	300	0.37	4.00	390	0.33	370	1.78	2	9.0	1.2	2.96	21.74	162
14	C3	6.42	300	0.37	4.00	390	0.33	370	1.78	3	13.5	1.2	2.96	21.74	162
15	C4	6.42	300	0.37	4.00	390	0.33	370	1.78	4	18.0	1.2	2.96	21.74	162
16	D0	7.00	385	0.41	4.00	390	0.27	275	2.06	0	0	0	0	23.54	180
17	D1	7.00	385	0.41	4.00	390	0.27	275	2.06	1	3.2	0	0	23.54	180
18	D2	7.00	385	0.41	4.00	390	0.27	275	2.06	2	6.4	0	0	23.54	180
19	D3	7.00	385	0.41	4.00	390	0.27	275	2.06	3	9.6	0	0	23.54	180
20	D4	7.00	385	0.41	4.00	390	0.27	275	2.06	4	12.8	0	0	23.54	180
21	E0	7.00	385	0.40	4.00	390	0.27	275	2.06	0	0	0.3	0.74	22.90	200
22	E1	7.00	385	0.40	4.00	390	0.27	275	2.06	1	3.2	0.3	0.74	22.90	200

Table 1Detail of Prisms Tested (contd.)

S.No	Specimen Designation	Lateral Reinforcement			Longitudinal reinforcement		Mesh Reinforcement					Steel Fiber		f_c' (Mpa)	ε_c' 10^{-5}
		Dia. (mm)	f_y (Mpa)	C_i	Dia. (mm)	f_y (Mpa)	Dia. (mm)	f_y (Mpa)	Spacing (mm)	No.of Layers	S_f	V_f %	RI		
23	E2	7.00	385	0.40	4.00	390	0.27	275	2.06	2	6.4	0.3	0.74	22.90	200
24	E3	7.00	385	0.40	4.00	390	0.27	275	2.06	3	9.6	0.3	0.74	22.90	200
25	E4	7.00	385	0.40	4.00	390	0.27	275	2.06	4	12.8	0.3	0.74	22.90	200
26	F0	7.00	385	0.40	4.00	390	0.27	275	2.06	0	0	0.9	2.21	23.00	195
27	F1	7.00	385	0.40	4.00	390	0.27	275	2.06	1	3.2	0.9	2.21	23.00	195
28	F2	7.00	385	0.40	4.00	390	0.27	275	2.06	2	6.4	0.9	2.21	23.00	195
29	F3	7.00	385	0.40	4.00	390	0.27	275	2.06	3	9.6	0.9	2.21	23.00	195
30	F4	7.00	385	0.40	4.00	390	0.27	275	2.06	4	12.8	0.9	2.21	23.00	195
31	G0	7.00	448	0.37	3.00	350	0.27	250	3.1	0	0	0	0	26.25	190
32	G2	7.00	448	0.37	3.00	350	0.27	250	3.1	2	3.79	0	0	26.25	190
33	G3	7.00	448	0.37	3.00	350	0.27	250	3.1	3	5.68	0	0	26.25	190
34	G4	7.00	448	0.37	3.00	350	0.27	250	3.1	4	7.58	0	0	26.25	190
35	H0	7.00	448	0.37	3.00	350	0.27	250	3.1	0	0	0.4	0.983	26.25	210
36	H2	7.00	448	0.37	3.00	350	0.27	250	3.1	2	3.79	0.4	0.983	26.25	210
37	H3	7.00	448	0.37	3.00	350	0.27	250	3.1	3	5.68	0.4	0.983	26.25	210
38	H4	7.00	448	0.37	3.00	350	0.27	250	3.1	4	7.58	0.4	0.983	26.25	210
39	I0	7.00	448	0.37	3.00	350	0.27	250	3.1	0	0	0.8	1.965	26.25	205
40	I2	7.00	448	0.37	3.00	350	0.27	250	3.1	2	3.79	0.8	1.965	26.25	205
41	I3	7.00	448	0.37	3.00	350	0.27	250	3.1	3	5.68	0.8	1.965	26.25	205
42	I4	7.00	448	0.37	3.00	350	0.27	250	3.1	4	7.58	0.8	1.965	26.25	205
43	J0	7.00	448	0.40	3.00	350	0.27	250	3.1	0	0	1.2	2.96	24.25	210
44	J2	7.00	448	0.40	3.00	350	0.27	250	3.1	2	3.79	1.2	2.96	24.25	210
45	J3	7.00	448	0.40	3.00	350	0.27	250	3.1	3	5.68	1.2	2.96	24.25	210
46	J4	7.00	448	0.40	3.00	350	0.27	250	3.1	4	7.58	1.2	2.96	24.25	210

Fig. 1. (a) Reinforcement details of the specimens

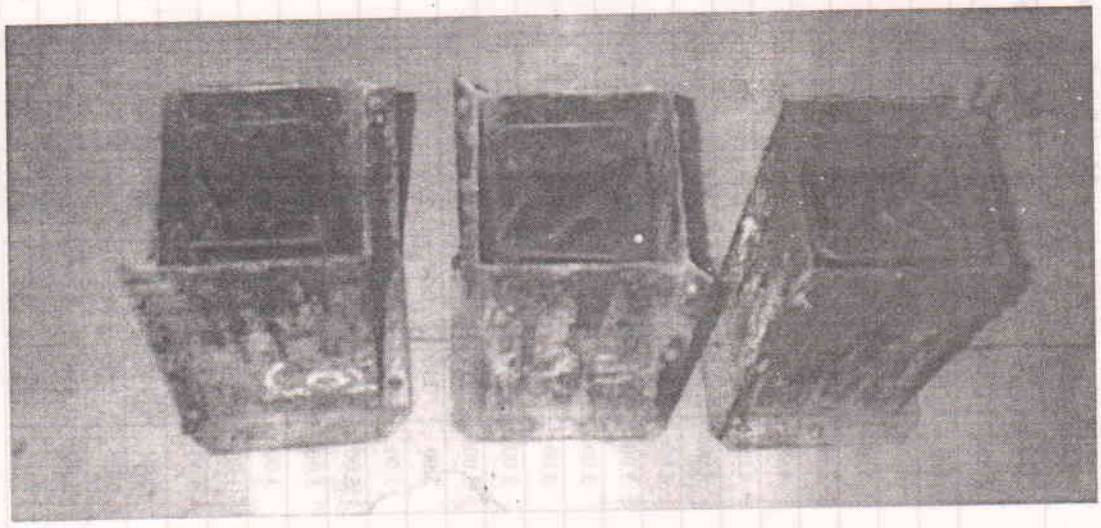

Fig. 1. (b) Molds used for casting the prisms

Casting of the specimen

The prepared cage of reinforcement was kept in molds carefully. Spacer rods of 2 mm diameter galvanized iron wires were kept temporarily in between the layers of mesh to maintain spacing between the layers. The prisms were cast in the vertical position. First, the gap between the mold and the reinforcement was filled to about half the height of the mold using cement mortar, and then fiber reinforced concrete was placed inside the mesh up to the same level. Then, a needle vibrator was used to compact the core fiber reinforced concrete. The mould was filled in three layers using the same technique. The top face of the prism specimen was capped with a rich cement paste. The specimens was demolded forty eight hours after casting and cured for twenty eight days in curing pond.

Testing

The cured specimens were capped with plaster of Paris before testing, to provide a smooth loading surface. A Tinius - Olsen testing machine of 1810 KN in capacity was used for testing the

prisms under axial compression. Specially fabricated compressometers suitable for prisms, which were fabricated by the earlier investigators [12] on confined concrete, were adopted, in measuring the deformations during loading. Fig. 2(a) shows the details of the compressometer attached to the specimen. Fig. 2(b) shows the photograph of the same arrangement.

The capped specimen with the compressometer attached was placed on the movable cross head of the testing machine, and tested under strain control rate of loading. The deformations were noted, and strains were calculated. Fig. 3 shows the test arrangement. The test was continued until the load dropped to about 75 to 80 % of the ultimate load in the post ultimate region for both confined and unconfined prism specimens.

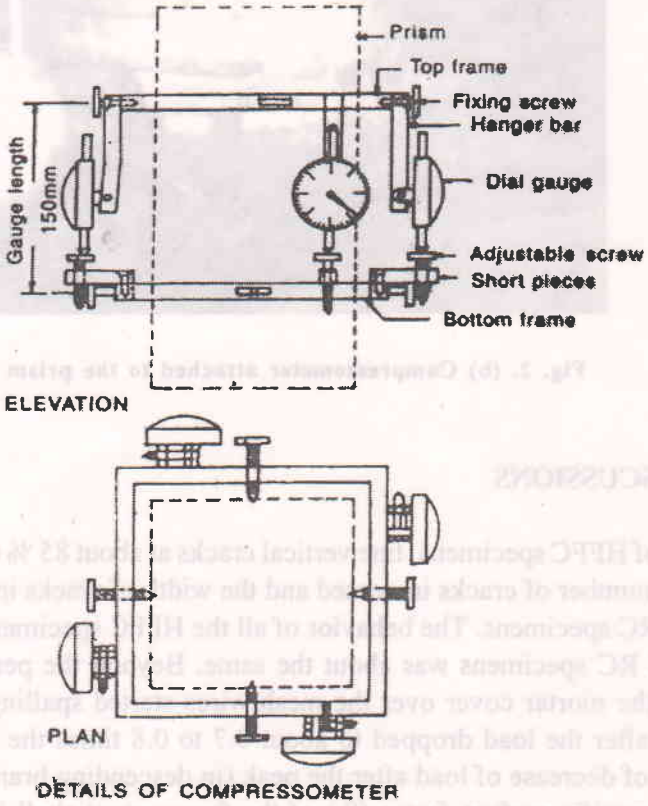

DETAILS OF COMPRESSOMETER

Fig. 2. (a) Detail of compressometer

Fig. 2. (b) Compressometer attached to the prism

RESULTS AND DISCUSSIONS

In the case of HFFC specimens, fine vertical cracks at about 85 % of the peak load. With the increase in load, the number of cracks increased and the width of cracks increased at a reduced rate compared to that of RC specimens. The behavior of all the HFFC specimens up to 85 % of the peak load of the confined RC specimens was about the same. Beyond the peak loads, the mesh wires started bulging and the mortar cover over the mesh wires started spalling. The extent of spalling became severe only after the load dropped to about 0.7 to 0.8 times the peak load. The extent of spalling and the rate of decrease of load after the peak (in descending branch of stress-strain curve) depended upon the specific surface factor (S_f) of the ferrocement shell if the tie confinement, as indicated by the confinement index (C_i) and the passive confinement of steel fiber indicated by the RI of FRC was the same. The higher the specific surface factor (S_f), the lower the rate of decrease of load and the extent of spalling. This may be due to the improvement of dimensional stability as well as the integrity of the material, caused by the presence of large specific surface factor of the ferrocement shell provided as additional confinement to the core fiber reinforced concrete.

The ultimate strength of HFFC, the corresponding strain and strain at 0.85 times the ultimate strength (after the peak) varied linearly with specific surface factor of the ferrocement shell for the same values of CI and RI. The predicted equation [16] fit for the same are

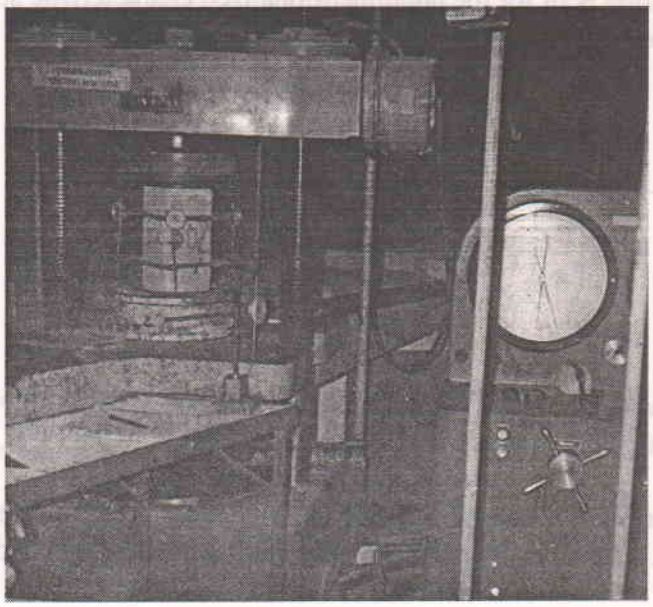

Fig. 3. Details of Specimen under test

$$P = f_c'(1 + 0.55C_i)\,(1.0228 + 0.1024\,RI)\,(1.0 + 0.0166\,S_f)\,A_g + f_y A_s \quad ...(1)$$

$$\varepsilon_{fu} = \varepsilon_c'(1.0 + 5.2C_i)\,(0.9899 + 0.2204\,RI)\,(1.0 + 0.1359S_f) \quad ...(2)$$

$$(\varepsilon_{0.85fu}/\varepsilon_u) = 2.1127 + 0.0338\,S_f \quad ...(3)$$

Experimental stress-strain curves

From observed data, for a given specimen, the longitudinal deformations were calculated from the average readings of the four dial gauges of the compressometer. As there was no severe spalling in HFFC specimens until the load dropped by about 20 to 25 % of peak load, the specimens were treated as dimensionally stable and hence the gross cross- sectional area was used in calculating the stress values. Stress-strain curves were drawn for three companion specimens of a set with the same origin, and an average curve was taken to represent the set. Such average curves for all the sets of one typical batch with a common origin are shown in Figs. 4.1 to 4.5.

An examination of the stress-strain diagrams for HFFC indicates that the behavior is similar for all specimens. The similarity leads to the conclusion that there is a unique shape of the stress - strain diagram, if expressed in nondimensional form, along both the axes. The said form is obtained by dividing the stress at any level by the stress at ultimate and the strain at any stress level by the strain at ultimate. By nondimensionalising the stress and strain as above the influence of specific surface factor (S_f), reinforcing index (RI) and confinement index (C_i) is eliminated for any specimen. Fig.5 shows the plot of characteristic value of non-dimensionalized stress (stress ratio) as ordinate and nondimensionalized strain (strain ratio) as abscissa. The plot indicates that the stress-strain behavior of HFFC can be represented by a general curve, which functions as a stress block.

The following equation is fit for the nondimensionalized characteristic stress-strain curve for HFFC in axial compression.

$$\frac{f}{f_u} = \left[\frac{A_1 \left(\frac{\varepsilon}{\varepsilon_{fu}} \right)}{1.0 + B_1 \left(\frac{\varepsilon}{\varepsilon_{fu}} \right) + C_1 \left(\frac{\varepsilon}{\varepsilon_{fu}} \right)^2} \right] \quad ...(4)$$

where,

For ascending portion of the stress - strain curve of HFFC; $A_1 = 6.852$, $B_1 = 4.852$, $C_1 = 1.0$
For descending portion of the stress - strain curve of HFFC; $A_1 = 2.833$, $B_1 = 0.833$, $C_1 = 1.0$

Two sets of constants are proposed because the ascending portion of stress-strain curves i.e., beyond ultimate portion a slow downward trend. The common boundary conditions used are:

(i) $$\text{At} \left(\frac{\varepsilon}{\varepsilon_{fu}} \right) = 1.0, \qquad \left(\frac{f}{f_u} \right) = 1.0 \quad ...(5)$$

(ii) $$\text{At} \left(\frac{\varepsilon}{\varepsilon_{fu}} \right) = 1.0, \qquad \frac{d\left(\frac{f}{f_u} \right)}{d\left(\frac{\varepsilon}{\varepsilon_{fu}} \right)} = 0.0 \quad ...(6)$$

Additional boundary conditions for ascending portion of stress-strain curve is:

(iii) $$\text{At} \left(\frac{\varepsilon}{\varepsilon_{fu}} \right) = 0.1, \qquad \left(\frac{f}{f_u} \right) = 0.458 \quad ...(7)$$

For descending portion of stress-strain curve,

(iv) $$\text{At} \left(\frac{\varepsilon}{\varepsilon_{fu}} \right) = 0.1, \qquad \left(\frac{f}{f_u} \right) = 0.458 \quad ...(8)$$

The condition (iii) and (iv) are obtained from the experimental data. At $(\varepsilon / \varepsilon_{fu}) = 0.1$, the curve deviates from the initial tangent and at $(\varepsilon / \varepsilon_{fu}) = 2.0$, the reduction in strength is 15%. Fig.6 indicates that the curve of the equation proposed passes close to all the experimental points.

Hence, the generalized stress-strain equation for HFFC can be written as

$$f = \left[\frac{A\varepsilon}{1.0 + B\varepsilon + C\varepsilon^2} \right] \qquad ...(9)$$

Where

$$A = A_1 \left(\frac{f_u}{\varepsilon_{fu}} \right) \qquad B = B_1 \left(\frac{1.0}{\varepsilon_{fu}} \right) \qquad C = C_1 \left(\frac{1.0}{\varepsilon_{fu}} \right)^2$$

The stress -strain equations proposed for HFFC is useful in developing stress block parameters required for computing the moment and curvature of HFFC sections.

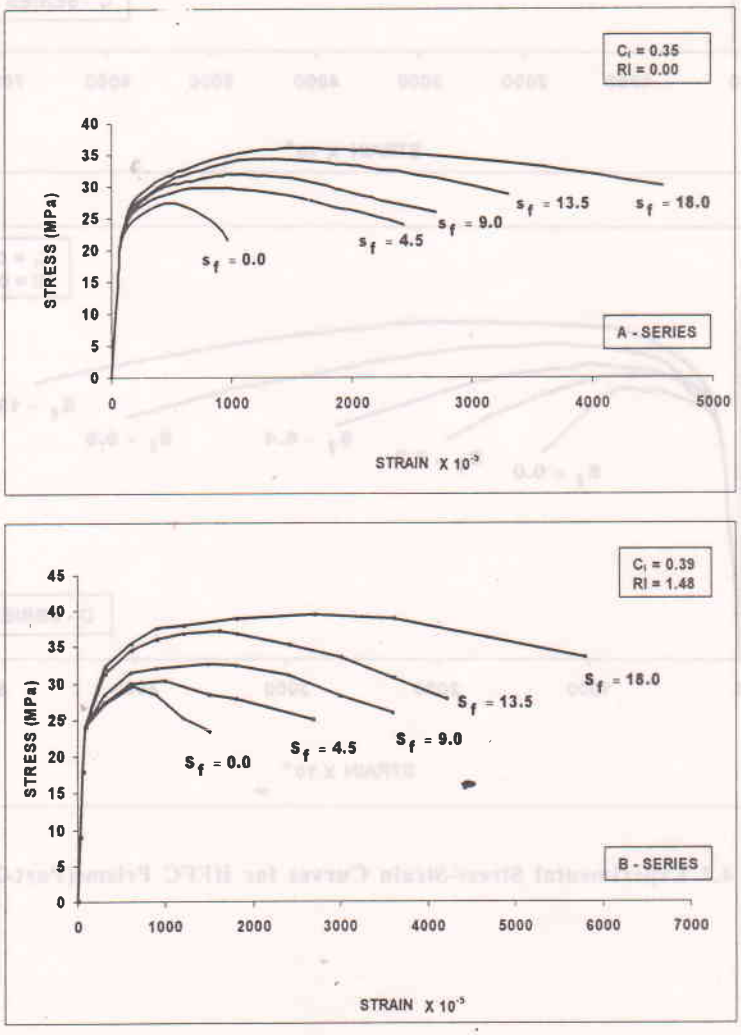

Fig. 4.1 Experimental Stress-Strain Curves for HFFC Prisms(Part-1)

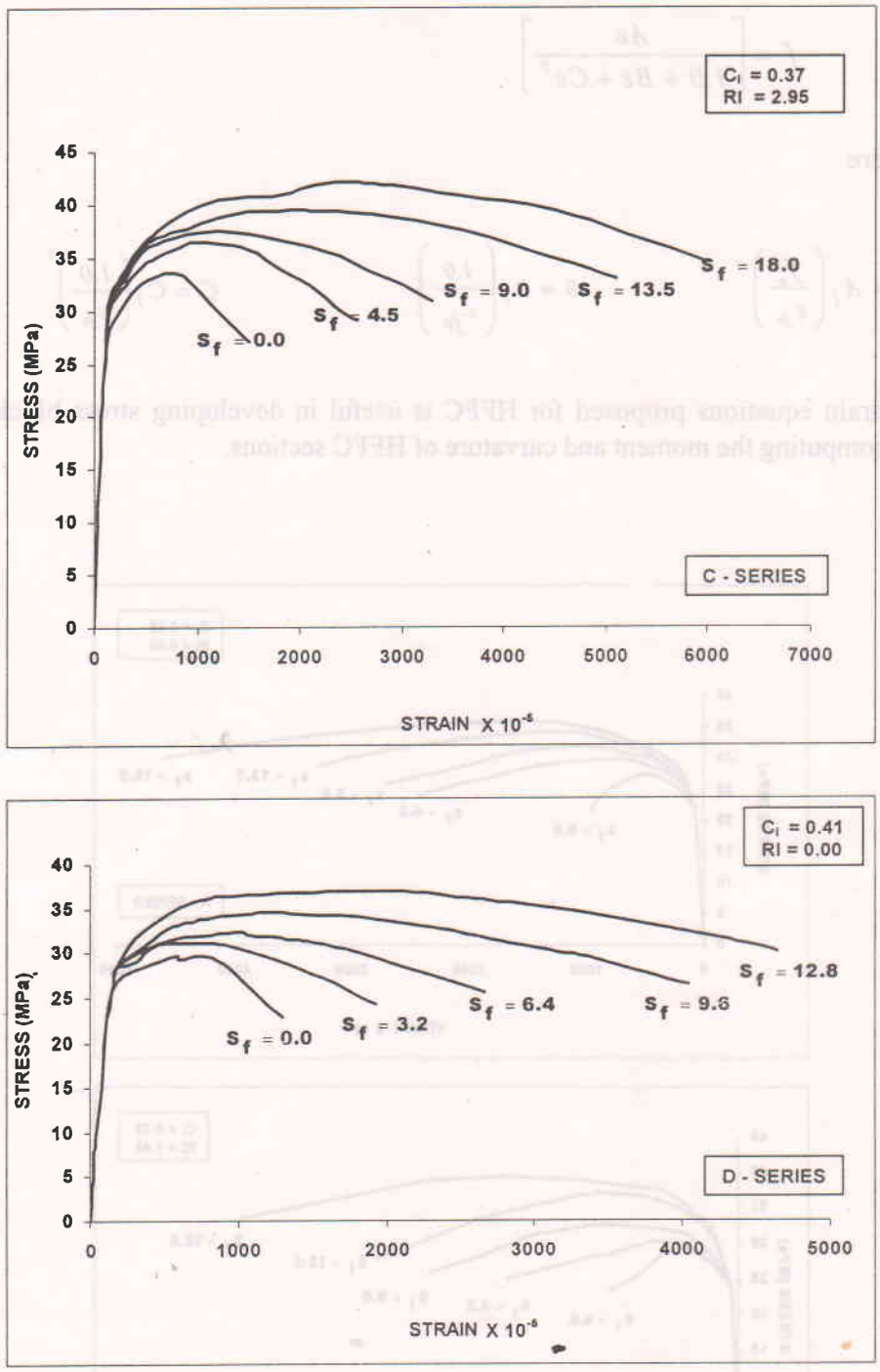

Fig. 4.2 Experimental Stress-Strain Curves for HFFC Prisms(Part-2)

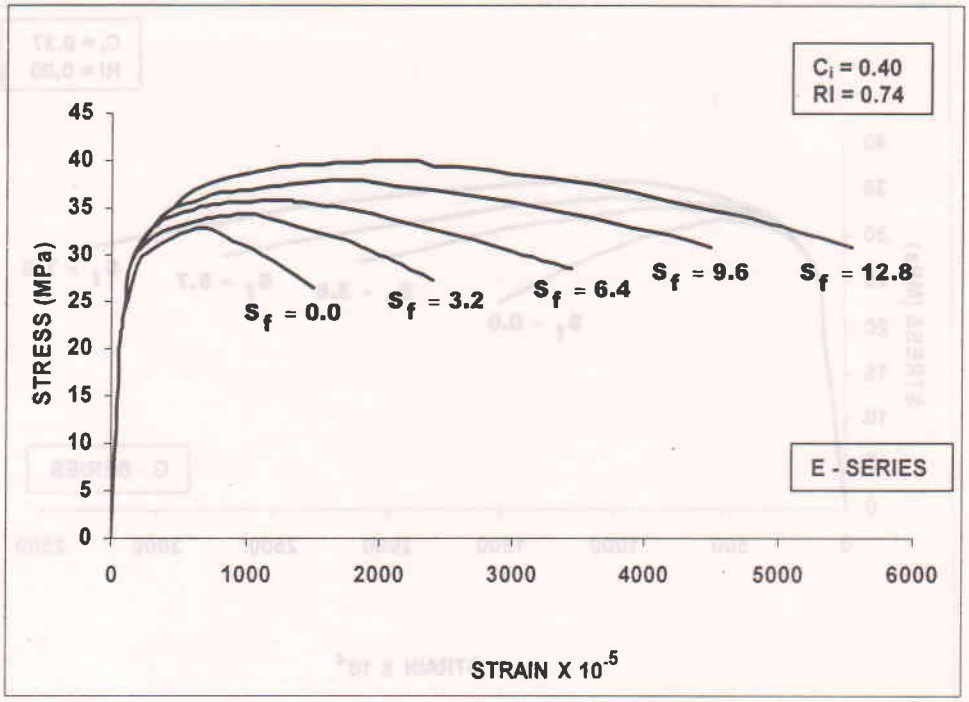

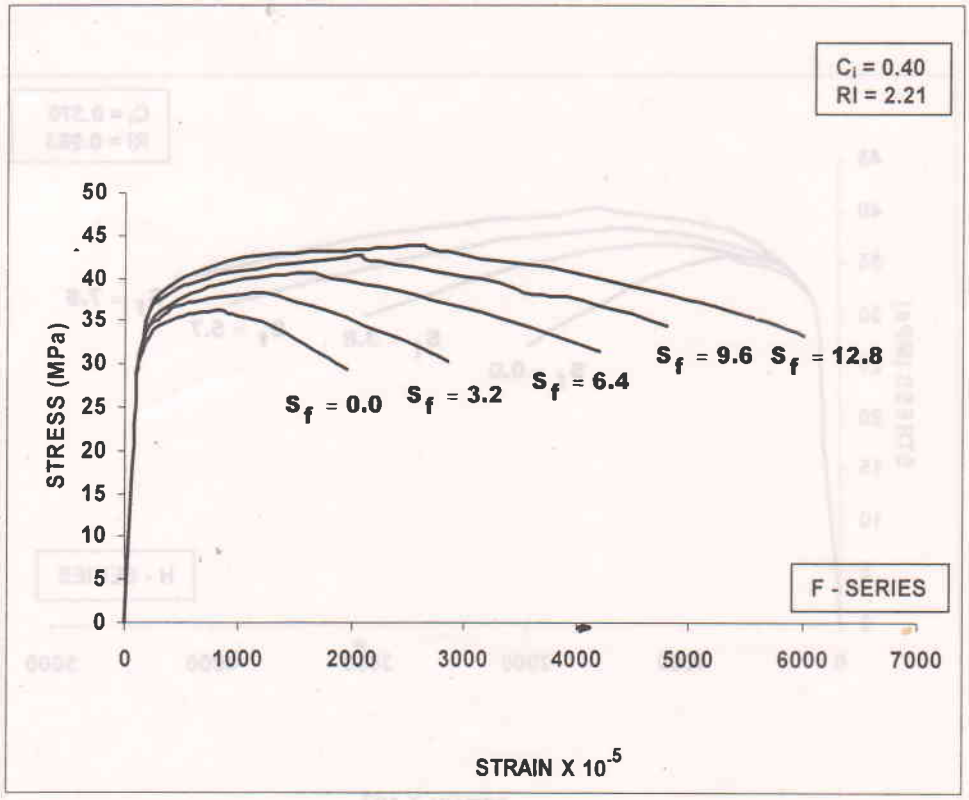

Fig. 4.3 Experimental Stress-Strain Curves for HFFC Prisms(Part-3)

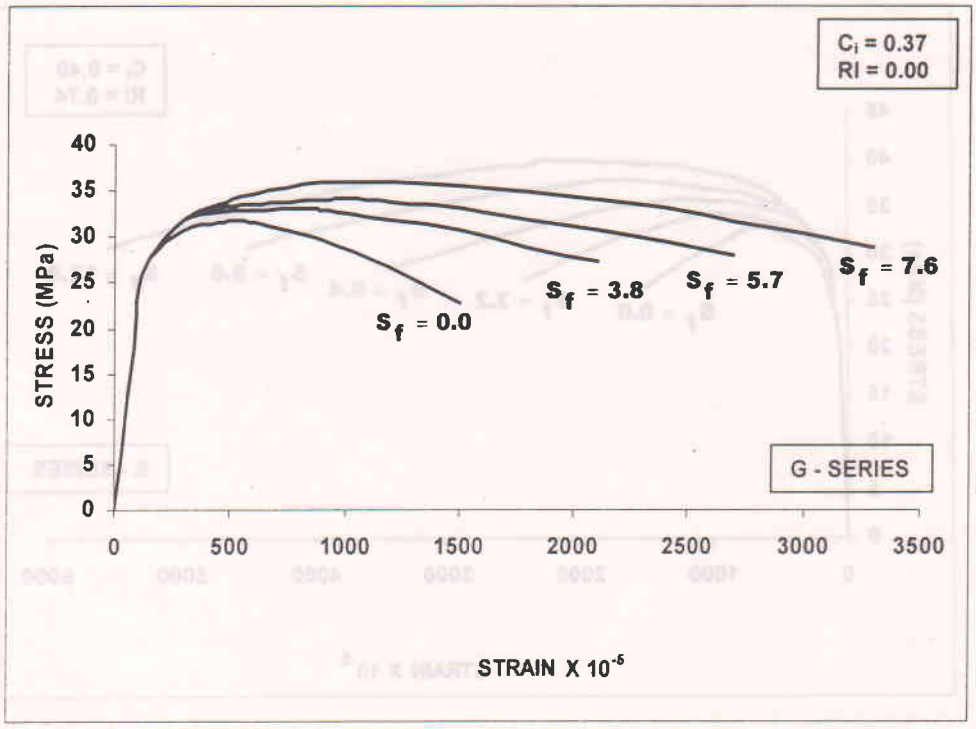

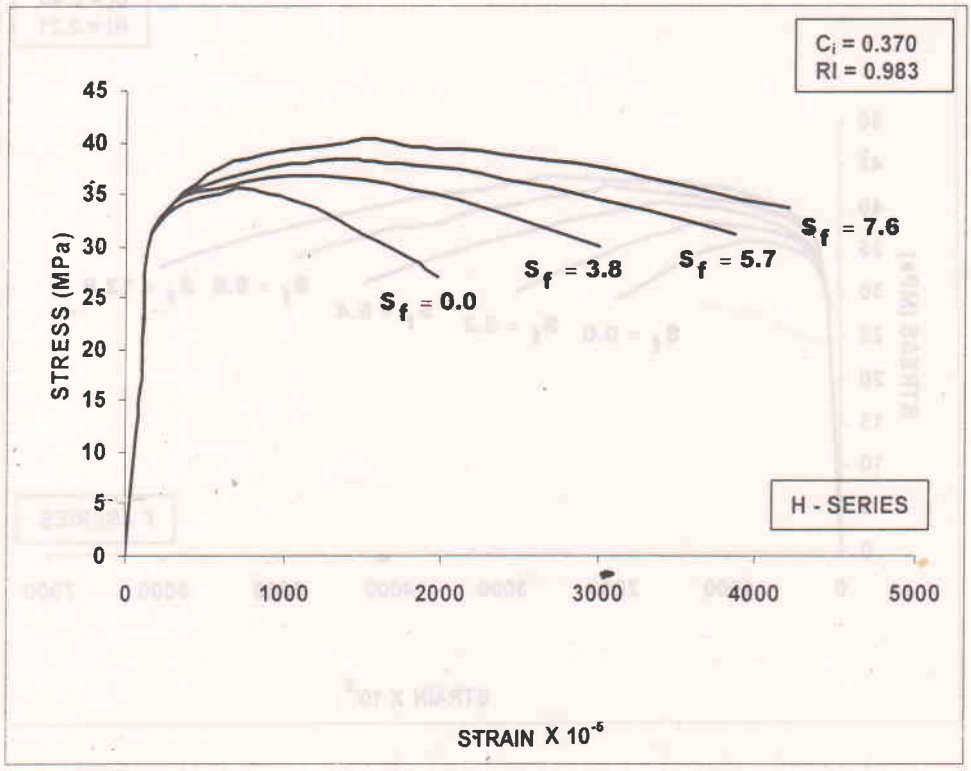

Fig. 4.4 Experimental Stress-Strain Curves for HFFC Prisms(Part-4)

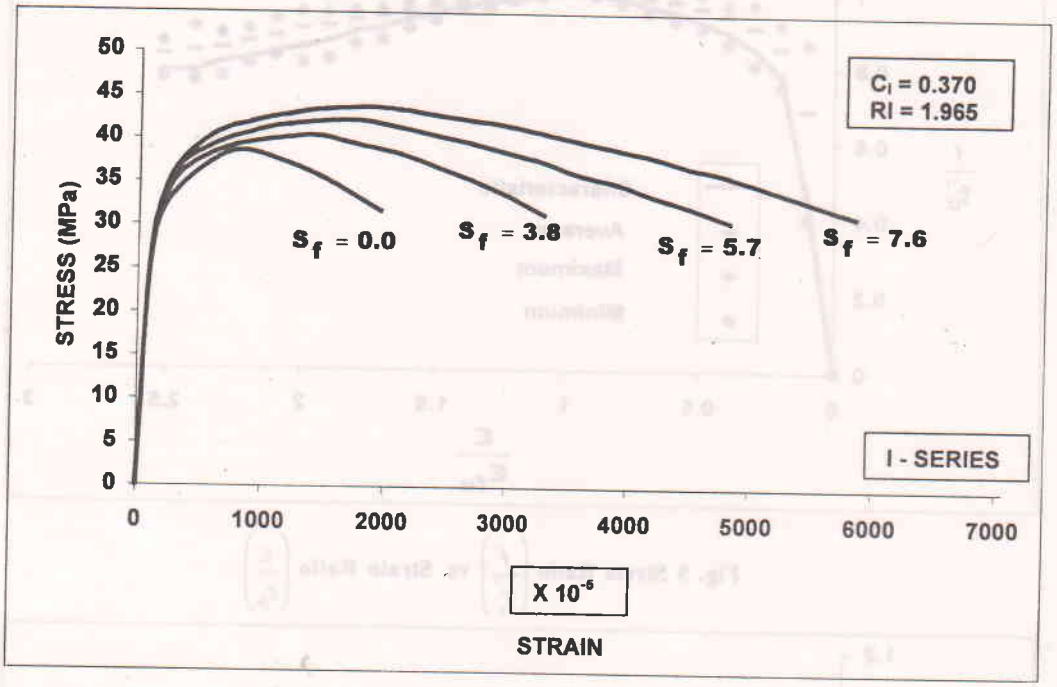

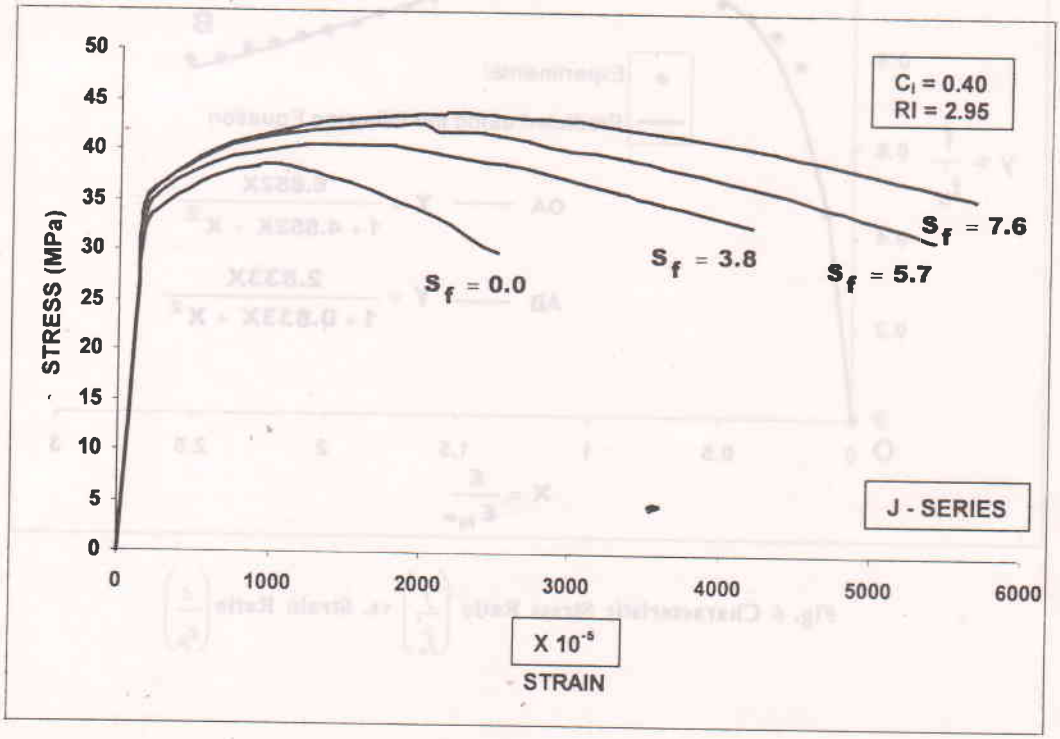

Fig. 4.5 Experimental Stress-Strain Curves for HFFC Prisms(Part-5)

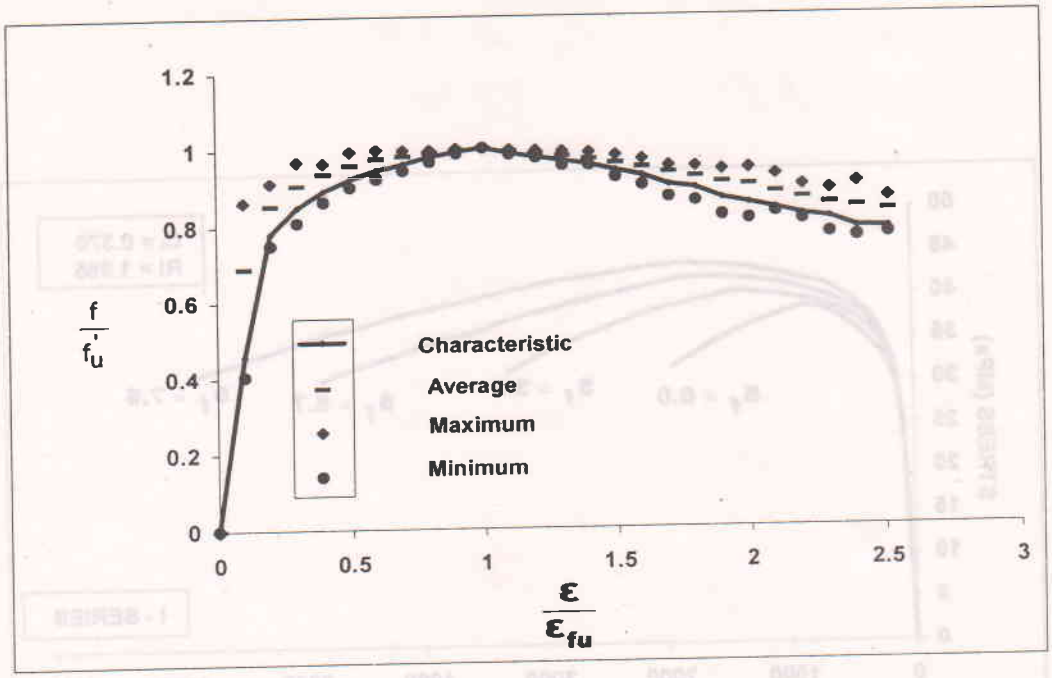

Fig. 5 Stress Ratio $\left(\frac{f}{f_u'}\right)$ vs. Strain Ratio $\left(\frac{\varepsilon}{\varepsilon_{fu}}\right)$

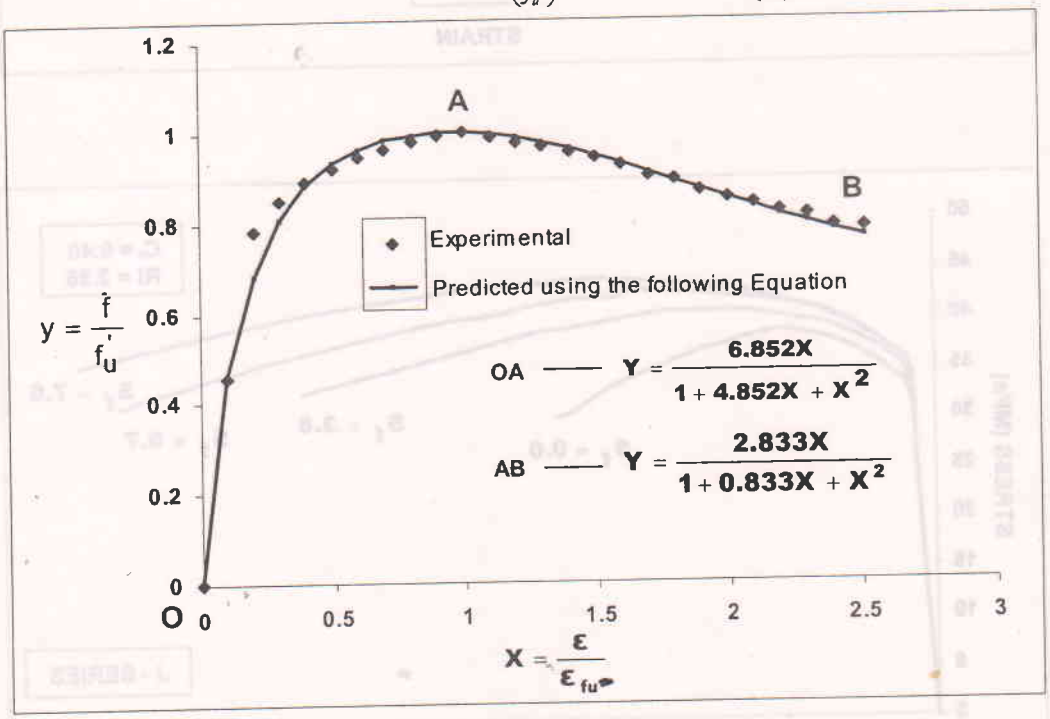

Fig. 6 Characteristic Stress Ratio $\left(\frac{f}{f_u'}\right)$ vs. Strain Ratio $\left(\frac{\varepsilon}{\varepsilon_{fu}}\right)$

CONCLUSIONS

The nondimensional characteristic stress-strain equation for HFFC is proposed which can be used to predict the constitutive behavior of HFFC in axial compression.

REFERENCES

1. Alsayed, S.H.1992, Confinement of Reinforced Concrete Columns by Rectangular Ties and Steel Fibers. *Magazine of Concrete Research*, 44(161): 265-270.
2. Ahmad, S.H.; and Shah, S.P.1982, Stress-strain curves of Concrete Confined by Spiral Reinforcement. *ACI Journal Proceedings*, 79(6): 484-490.
3. Blume, J.A., et al., 1961, Design of multistory reinforced concrete buildings for earthquake motions. Portland Cement association, USA.
4. Ganesan, N; and Anil, J. 1993. Strength and behavior of RC columns confined by ferrocement. *Journal of Ferrocement*, 23(2): 99-108.
5. Ganesan, N; Ramanamurthy, J.V.1990. Strength and behavior of confined steel fiber reinforced concrete columns. *ACI Materials Journal*, 87(3): 221-227.
6. IS 456 – 2000. *Indian Standard Code of Practice for Plain and Reinforced Concrete*. Delhi: Indian Standards.
7. IS 8112 – 1981. *Specifications for 43 Grade Ordinary Portland Cement*. Delhi: Indian Standards.
8. Pama, R.P.; Robles-Austriaco, L.R.; and Rubio-Hermosura, N. 1993. Current researches on ferrocement. *Journal of Ferrocement*, 23(4): 227-288.
9. Paulay and Priestley, M.J.N. 1992. *Seismic Design of Reinforced Concrete Concrete and Masonry Buildings*. New York: John Wiley and Sons.
10. Reddy, S.R. 1974. Behavior of Concrete Confined in Rectangular Binders and its Applications in Flexure of Reinforced Concrete Structures, Ph.D. Thesis, J.T.University, Hyderabad, India.
11. Rao, C.B.K. and Rao, A.K. 1986. Stress strain curve in axial compression and Poisson's ratio of ferrocement. *Journal of Ferrocement*, 16(2): 117-128.
12. Rao, A.K.; Reddy, K.N.; and Reddy, V.M. 1979. Effect of stirrup confinement on flexural behavior of prestressed concrete beams. *Journal of IE(India)* 59: 258-266.
13. Ramesh, K.; Seshu, D.R.; and Prabhakar, M. 2000. A study of tie confined fiber reinforced concrete under axial compression. *RILEM Journal of Concrete Science and Engineering*, 02: 230-236.
14. Ramesh, K.; Seshu, D.R.; and Prabhakar, M. 2000. Confined fiber reinforced concrete (CFRC). *Proceedings of Twenty Fifth Anniversary International Conference on Our World in Concrete and Structures*, 531-537. Singapore: CI – Premier Pvt. Ltd.
15. Seshu, D.R., and Rao, A.K. 1998. Behavior of ferrocement confined reinforced concrete(FCRC) under axial compression. *RILEM Materials and Structures Journal*, 31: 628-633.
16. Ramesh, K.; Seshu, D.R.; and Prabhakar, M. 2002. Behavior of Hybrid Ferro Fiber Concrete (HFFC) under Axial Compression. *Journal of Ferrocement*, 32(3): 233-249.